$$Q(\alpha, \beta, J, \mu) = \pi f(\vec{r}, v)/m^2 \quad (2)$$

is conserved along the bounce-averaged convection trajectory, where α, β are the Euler potentials for labeling field lines, μ, J are the first and second invariants, and f is the standard phase space density. An equivalent description in terms of the particle total energy is [eq. 41, *Northrop and Teller,* 1960],

$$n(\vec{r}, W, \mu) = 2BQ/v_{\|} \quad (3)$$

where W is the total energy defined above, $v_{\|}$ is the parallel velocity, and n is the number of particles in d^3r at a given value of W, μ.

3 Algorithms and Results

To carry out this method for any K or equatorial pitch angle, we need an algorithm for calculating the functional dependence of $B_m(K)$ on K. We do this numerically, (Figure 3), first mapping the field line from the equator to the ionosphere, here showing several longitudes collapsed into one display. We numerically integrate these B(s) curves to obtain the second adiabatic invariant K(s). Note that on the day side, there are field lines which do not have a minimum at the equator, and thus K is undefined (imaginary) over some range of s. *Northrop and Teller* [1960] discuss this phenomenon, and like them, we find a generalized form of K defined as the sum of all non-imaginary K's along a field line. With that definition, we calculate K from the minimum, either at the equator or elsewhere, to get K(s). With these two quantities, we can now calculate $B_m(K)$ as a polynomial expression, plotted in the final panel. We use 10th degree polynomials and arrive at an expression with less than 3% maximum deviation. Note that this is just an automated way of carrying out the Taylor and Hones graphical method, which we independently derived.

This part of the algorithm is the most time consuming, taking 5 hours on a SUN IPC for solving a 100 x 100 grid of the equatorial plane and using 200 integration steps along a field line. Once the polynomials are initialized, calculating a total energy for arbitrary K and μ, which gives simultaneously every spatially distinct trajectory in the equatorial plane, required only 30 seconds, or only 3 seconds if μ alone changes. This is to be contrasted with 3 minutes per single particle trace using a predictor-corrector method to time-integrate the forces.

Now that we have a realistic B(K) mapping, we also need to make U more realistic as well. *Pinto et al.* [1987] showed that drift trajectories would be greatly influenced by the ionospheric dynamo electric field [*Richmond et al.,* 1980]. This dynamo field strengthens convection at low L-shells and compensates for the Volland-Stern shielding. However, the field is quadrupolar and topologically different from the dipolar Volland-Stern field, so that (Figure 2) in real space the tangent lines form a loop at low altitudes. When mapped into UB(K) space, the loop becomes a pleat, but only in the night half of the magnetosphere.

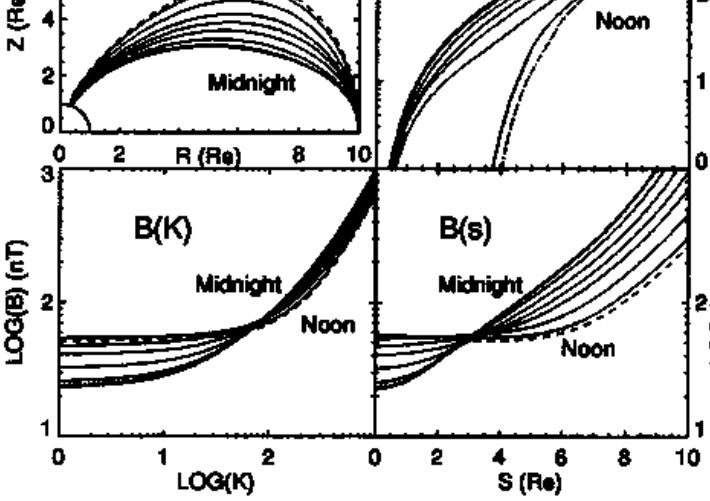

Fig. 3: a) Fieldlines traced from equatorial plane at 1 Re with longitude varying from midnight to noon in 20 increments; b) K(s) for fieldlines at 10 Re; c) B_m(K), whic is well defined for all fieldlines; and d) B(s) for fieldlines a 10 Re with an off equatorial minimum in the noon fieldlin

Since this is the first time trajectories have been show for these realistic fields, we plot some examples in Figur 4. In panel (a), we see that for K=0 or 90° equatoria pitch angles at a magnetic moment of 0.01 keV/nT, ther are closed drift trajectories that do not encircle the eart [e.g., *Chen,* 1970], called "banana" orbits after tokoma usage [*Strangeway and Johnson,* 1984]. In UB(K) space these orbits are straight lines that nest in a concavity o the lower tangency curves. Note that the extra loop sup ports a new class of banana orbits; however these banan orbits are inside normal, earth encircling trapped orbits and thus have no access to the open drift trajectories fron the tail. In panel (b), we see that for K=100, the banan orbits merge and appear outside the normal trapped orbi region. This allows them to be readily filled by diffusion o Coulomb drag effects. More importantly, there exists a open drift orbit threading between the normal closed or bits and the banana orbits. Because of the large value of I at low altitudes, convecting tail particles on this open drif trajectory become more pancake-like as the pitch angle ro tates toward 90°, panel (c), and equatorial $n(\vec{r}_{eq}, W, \mu)$ in creases. Panel (d) plots the change in $B_{eq}/\sqrt{\mu(B_m - B_{eq})}$ which is directly proportional to the change in $n(\vec{r}_{eq}, W, \mu)$ Since this orbit is open to the tail, unlike its near neigh bors, it alone experiences an order of magnitude increas in $n(\vec{r}_{eq}, W, \mu)$ for some specific range of W, μ. This mecha nism can explain the peaks seen in this vicinity by ISEE-I [*Williams and Frank,* 1984, *Sheldon,* 1993].

Acknowledgments. This work was supported by gran NAG-5-1558. We benefitted from many helpful discussion with M. Collier, S. Christon, T. Eastman, M. Greenspan T. Birmingham and especially, T. Northrop. We especially thank the referee who brought the Taylor and Hones articl to our attention and for many helpful comments.